iScience

CellPress
OPEN ACCESS

Article

Epigenetic repression of *Cend1* by lysine-specific demethylase 1 is essential for murine heart development

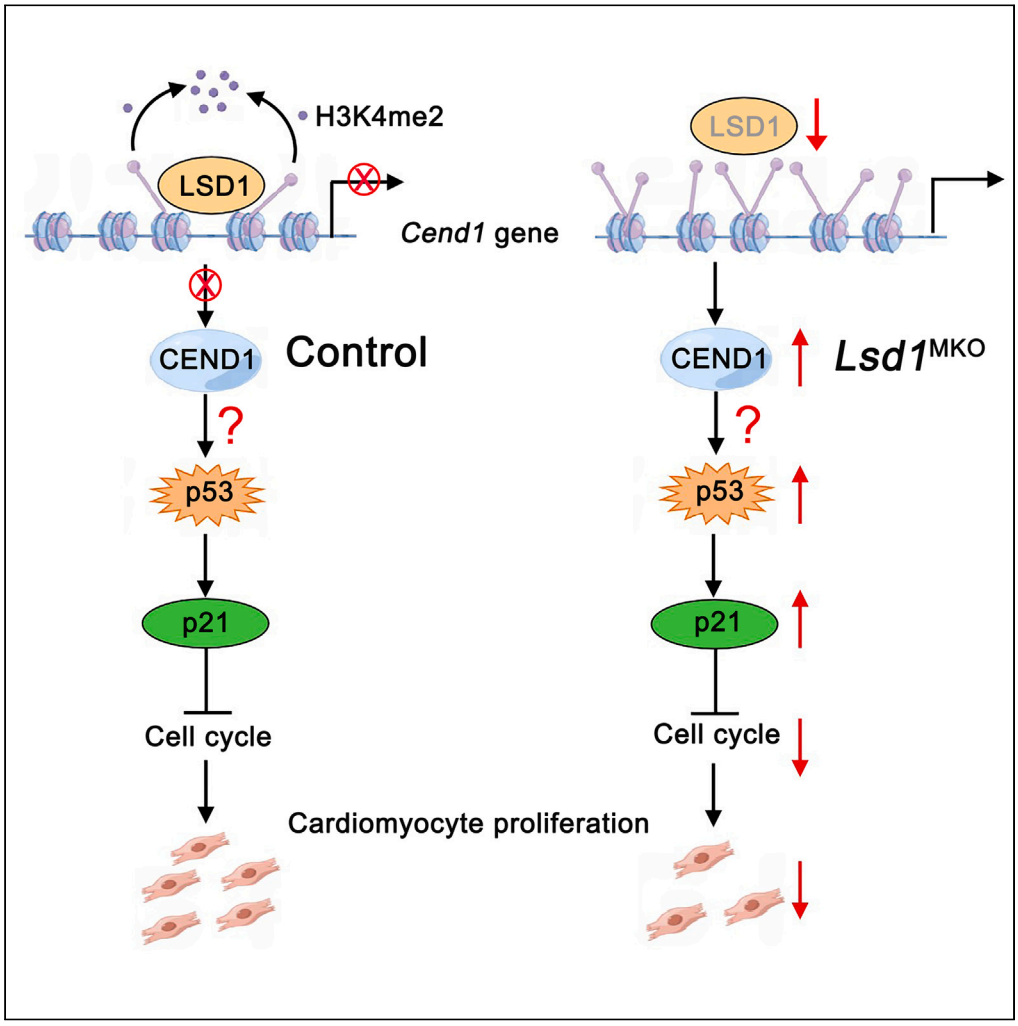

Huahua Liu, Rui Zhou, Shanshan Li, ..., Bin Zhou, Zuyi Yuan, Yidong Wang

zuyiyuan@mail.xjtu.edu.cn (Z.Y.)
yidwang119@xjtu.edu.cn (Y.W.)

Highlights

LSD1 is essential for embryonic and neonatal heart development in mice

LSD1-dependent suppression of CEND1 supports cardiomyocyte proliferation

LSD1 represses *Cend1* transcription by erasing H3K4me2 at its promoter

LSD1-CEND1 axis regulates the proliferation of hiPSC-CMs

Liu et al., iScience *27*, 108722
January 19, 2024
https://doi.org/10.1016/j.isci.2023.108722

iScience

CellPress
OPEN ACCESS

Article

Epigenetic repression of *Cend1* by lysine-specific demethylase 1 is essential for murine heart development

Huahua Liu,[1,2,9] Rui Zhou,[3,9] Shanshan Li,[1,9] Jinling Dong,[2] Yuan Fang,[2] Yuru Luo,[2] Hongyu Su,[2] Baochang Lai,[2] Lingli Liang,[4] Donghong Zhang,[5] Yanmin Zhang,[3] John Y-J. Shyy,[6] Bin Zhou,[7] Zuyi Yuan,[1,*] and Yidong Wang[8,10,*]

SUMMARY

Epigenetic regulation of heart development remains incompletely understood. Here we show that LSD1, a histone demethylase, plays a crucial role in regulating cardiomyocyte proliferation during heart development. Cardiomyocyte-specific deletion of *Lsd1* in mice inhibited cardiomyocyte proliferation, causing severe growth defect of embryonic and neonatal heart. *In vivo* RNA-seq and *in vitro* functional studies identified *Cend1* as a target suppressed by LSD1. *Lsd1* loss resulted in elevated *Cend1* transcription associated with increased active histone mark H3K4me2 at *Cend1* promoter. *Cend1* knockdown relieved the cell-cycle arrest and proliferation defect caused by LSD1 inhibition in primary rat cardiomyocytes. Moreover, genetic deletion of *Cend1* rescued cardiomyocyte proliferation defect and embryonic lethality in *Lsd1* null embryos. Consistently, LSD1 promoted the cell cycle of cardiomyocytes derived from human-induced pluripotent stem cells by repressing CEND1. Together, these findings reveal an epigenetic regulatory mechanism involving the LSD1-CEND1 axis that controls cardiomyocyte proliferation essential for murine heart development.

INTRODUCTION

Cardiomyocyte proliferation drives myocardial growth during embryonic and neonatal heart development, which is essential for normal embryogenesis and postnatal growth.[1] Cardiomyocyte cell cycle is controlled by genetic and epigenetic regulators. In the past decades, many genetic factors, such as GATA4,[2] TBX20,[3] BRG1,[4] YAP,[5,6] GP130,[7] ERBB2,[8] PITX2,[9] MEIS1,[10] AGRIN,[11] and LRP6[12] have been found to regulate cardiomyocyte proliferation during heart development. In addition to genetic factors, epigenetic factors or mechanisms are also indicated in cardiomyocyte proliferation. Assay for Transposase Accessible Chromatin with high-throughput sequencing (ATAC-seq) demonstrates that chromatin condensation at the promoter regions of cell-cycle genes is associated with cell-cycle arrest of cardiomyocytes.[13] Retinoblastoma gene (RB) proteins can recruit heterochromatin protein 1 (HP1) to the promoter of cell-cycle genes and initiate heterochromatin formation, leading to the reduced transcription of these genes and consequently cell-cycle arrest of cardiomyocytes.[14] RB proteins also recruit HDAC1 to E2F-regulated promoters to deacetylate and inactivate cell-cycle genes.[15] Despite these previous findings, genetic and epigenetic regulations of cardiomyocyte proliferation remain incompletely understood. Identifying the new regulators is also clinically relevant in that they may serve as therapeutic targets for heart regeneration.

Lysine-specific demethylase 1 (LSD1, also known as KDM1A) is the first identified member of the demethylase family that removes mono- and di-methylated lysine on histone 3 (H3K4me1/2 and H3K9me1/2), which promotes and inhibits gene transcription, respectively.[16,17] Accumulating evidence shows that LSD1 is overexpressed in multiple types of cancers and promotes tumor cell proliferation.[18–22] As a result, LSD1 is currently a new candidate drug target for treating cancers in clinical trials.[23,24] Much less is known about the roles of LSD1 in cardiomyocyte proliferation during heart development. Germline deletion of *Lsd1* in mice leads to embryonic lethality before E7.5,[25] indicating an essential role of LSD1 in embryogenesis. A hypomorphic LSD1 allele has been reported to cause ventricular septal defect (VSD), suggesting its essential

[1]Department of Cardiology, First Affiliated Hospital, Cardiometabolic Innovation Center of Ministry of Education, Xi'an Jiaotong University, Xi'an, China
[2]The Institute of Cardiovascular Sciences, School of Basic Medical Sciences, Xi'an Jiaotong University, Xi'an, China
[3]Key Laboratory of Precision Medicine to Pediatric Diseases of Shaanxi Province, Shaanxi Institute for Pediatric Diseases, Xi'an Children's Hospital, Affiliated Children's Hospital, Xi'an Jiaotong University, Xi'an, China
[4]Department of Physiology and Pathophysiology, School of Basic Medical Sciences, Xi'an Jiaotong University, Xi'an, China
[5]Department of Cardiology, The Second Affiliated Hospital, Wenzhou Medical University, Wenzhou, China
[6]Division of Cardiology, Department of Medicine, University of California, San Diego, CA, USA
[7]Department of Genetics, Albert Einstein College of Medicine, New York, NY, USA
[8]The Institute of Cardiovascular Sciences, School of Basic Medical Sciences, Department of Cardiology, First Affiliated Hospital, Key Laboratory of Environment and Genes Related to Diseases of Ministry of Education, Cardiometabolic Innovation Center of Ministry of Education, Xi'an Jiaotong University, Xi'an, China
[9]These authors contributed equally
[10]Lead contact
*Correspondence: zuyiyuan@mail.xjtu.edu.cn (Z.Y.), yidwang119@xjtu.edu.cn (Y.W.)
https://doi.org/10.1016/j.isci.2023.108722

roles in heart development via undefined mechanisms.[26] The roles and mechanisms of LSD1 in regulation of heart development warrants further study.

In this study, using a mouse model with the cardiomyocyte-specific deletion of *Lsd1*, we find that LSD1 is essential for cardiomyocyte proliferation during embryonic and neonatal heart development. The underlying mechanism involves the LSD1 promotion of cardiomyocyte cell cycle progression by suppressing CEND1 (cell cycle exit and neuronal differentiation 1). LSD1 inhibits *Cend1* transcription by erasing the active histone mark H3K4me2 at its promoter. These findings demonstrate a previously unknown epigenetically regulated LSD1-CEND1 axis underlying cardiomyocyte proliferation during heart development, informing regenerative medicine for potential heart repair.

RESULTS

Lysine-specific demethylase 1 expression coincides with cardiomyocyte proliferation

To determine the role of LSD1 in heart development, we first examined the expression of LSD1 in embryonic and postnatal mouse hearts. The mRNA level of *Lsd1* was high at embryonic day 16.5 (E16.5) and postnatal day 1 (P1), and largely diminished after P7 (Figure S1A). A similar expression pattern was observed for LSD1 protein on Western blot and immunostaining (Figures S1B and S1C). Notably, on EdU labeling, the cardiomyocytes were highly proliferative at E16.5 and P1, when they expressed a high level of LSD1 (Figures S1A–S1D). In contrast, the cardiomyocytes were minimally proliferative after P7 when they expressed a low level of LSD1 (Figures S1A–S1D). Together, the elevated LSD1 expression along with cardiomyocyte proliferation suggests that LSD1 may participate in cardiomyocyte proliferation during heart development.

Lysine-specific demethylase 1 is prerequisite for embryonic cardiomyocyte proliferation

To determine the role of LSD1 in heart development, we crossed $Lsd1^{f/f}$ mice with $cTnT^{Cre}$ mice to generate a cardiomyocyte-specific *Lsd1* knockout mouse line ($Lsd1^{f/f}$;$cTnT^{Cre}$, hereafter refers to $Lsd1^{MKO}$), and their littermates ($Lsd1^{f/f}$ or $Lsd1^{f/+}$) were used as controls. *Lsd1* was efficiently and specifically deleted in cardiomyocytes at both mRNA and protein levels (Figures 1A and S2A–S2C). More than 90% of $Lsd1^{MKO}$ embryos were embryonic-lethal, and the remaining ones died shortly after birth (Figure 1B). The hearts of $Lsd1^{MKO}$ embryos were smaller than controls beginning at E10.5 (Figure 1C). They became dilated after E14.5 (Figure 1C), indicating of heart failure, which might contribute to the lethal phenotype. Histologic analysis showed that LSD1 loss severely impeded the myocardial development, as evidenced by the thin ventricle free wall (Figure 1D). In contrast, the trabecular myocardium was comparable between control and $Lsd1^{MKO}$ embryos (Figure S2D). Consistent with the previous report by *Nicholson* et al.,[26] $Lsd1^{MKO}$ embryos exhibited ventricular septal defect (Figure S2E). In line with the thin ventricular wall phenotypic feature, LSD1 loss greatly inhibited the cardiomyocyte proliferation, as revealed by EdU labeling (a marker of DNA synthesis) and immunostaining of pH3 (a marker of mitosis) and Aurora B (a marker of cytokinesis) (Figures 1E, S2F, and S2G). In contrast, TUNEL assays revealed that there was no apparent apoptosis of cardiomyocytes in control and $Lsd1^{MKO}$ embryos (Figure S2G). These results indicate that LSD1 is required for embryonic cardiomyocyte proliferation and myocardial growth.

Lysine-specific demethylase 1 is essential for neonatal cardiomyocyte proliferation

To determine the role of LSD1 in neonatal myocardial development, we selectively deleted *Lsd1* in cardiomyocytes by injecting AAV9-cTntCre virus into the heart of $Lsd1^{f/f}$ mice at postnatal day 1 (P1). The deletion of *Lsd1* severely restricted the heart and body growth of neonates (Figures 2A and 2B). Although the ratio of heart to body weight was comparable, mice with *Lsd1* deletion had reduced heart weight as compared to control mice (Figure 2C). Consistently, *Lsd1* deletion significantly reduced cardiomyocyte proliferation revealed by immunostaining of Ki67 (a proliferation marker) and pH3 (Figure 2D). In line with these findings, the pharmacological inhibition of LSD1 by GSKLSD1 repressed the proliferation of cultured neonatal rat and mouse cardiomyocytes as well as cardiomyocyte cell line H9C2 (Figures 2E–2G). Together, these results demonstrate that LSD1 is essential for neonatal cardiomyocyte proliferation and heart development.

Lysine-specific demethylase 1 inhibits *Cend1* transcription by erasing H3K4me2

To identify the downstream targets of LSD1, we used RNA-seq analysis of heart ventricles tissues from E12.5 control and $Lsd1^{MKO}$ embryos. This analysis revealed totally 367 differentially expression genes (DEGs). Among them, 291 were upregulated and 76 downregulated caused by LSD1 loss (Figures 3A and S3A), indicating LSD1 might act as a transcriptional repressor during heart development. Among the top 10 upregulated genes, *Tesc*,[27] *Meioc*,[28] *Trpv2*[29] and *Cend1*,[30] have been reported to negatively regulate cell cycle and cell proliferation (Figure S3B). Furthermore, Gene Ontology (GO) analysis indicated that the upregulated genes were largely involved in the negative regulation of cell proliferation (Figure S3C). In line with the results of GO analysis, Gene Set Enrichment Analysis (GSEA) demonstrated that the DEGs were enriched in cell cycle regulation pathways, including targets of E2F, G2M and Myc (Figure S3D). From GO and GSEA results as well as known functions, we selected 31 genes as candidate targets of LSD1 (Figure S3E); 23 genes were confirmed by qPCR (Figures 3B and S4A). To further verify the LSD1 regulation of these genes, we treated neonatal rat and mouse cardiomyocytes as well as H9C2 cells with LSD1 inhibitor GSKLSD1 and then examined changes in transcription. Consistent with findings from *in vivo* experiments, *Cend1, Meioc, Slf2* were significantly upregulated by the inhibition of LSD1 (Figures 3C and S4B). Conversely, overexpression of LSD1 decreased the expression of *Meioc* and *Cend1* (Figures 3D and S4C). Because *Cend1* is known to suppress neuronal progenitor cell proliferation and promote differentiation,[30] we hypothesized that LSD1 may promote cardiomyocyte proliferation by repressing *Cend1*. Thus, we used immunostaining to verify the upregulation of CEND1 protein in hearts of E12.5 $Lsd1^{MKO}$ embryos (Figure 3E). In addition, *Lsd1* deletion in neonatal cardiomyocytes

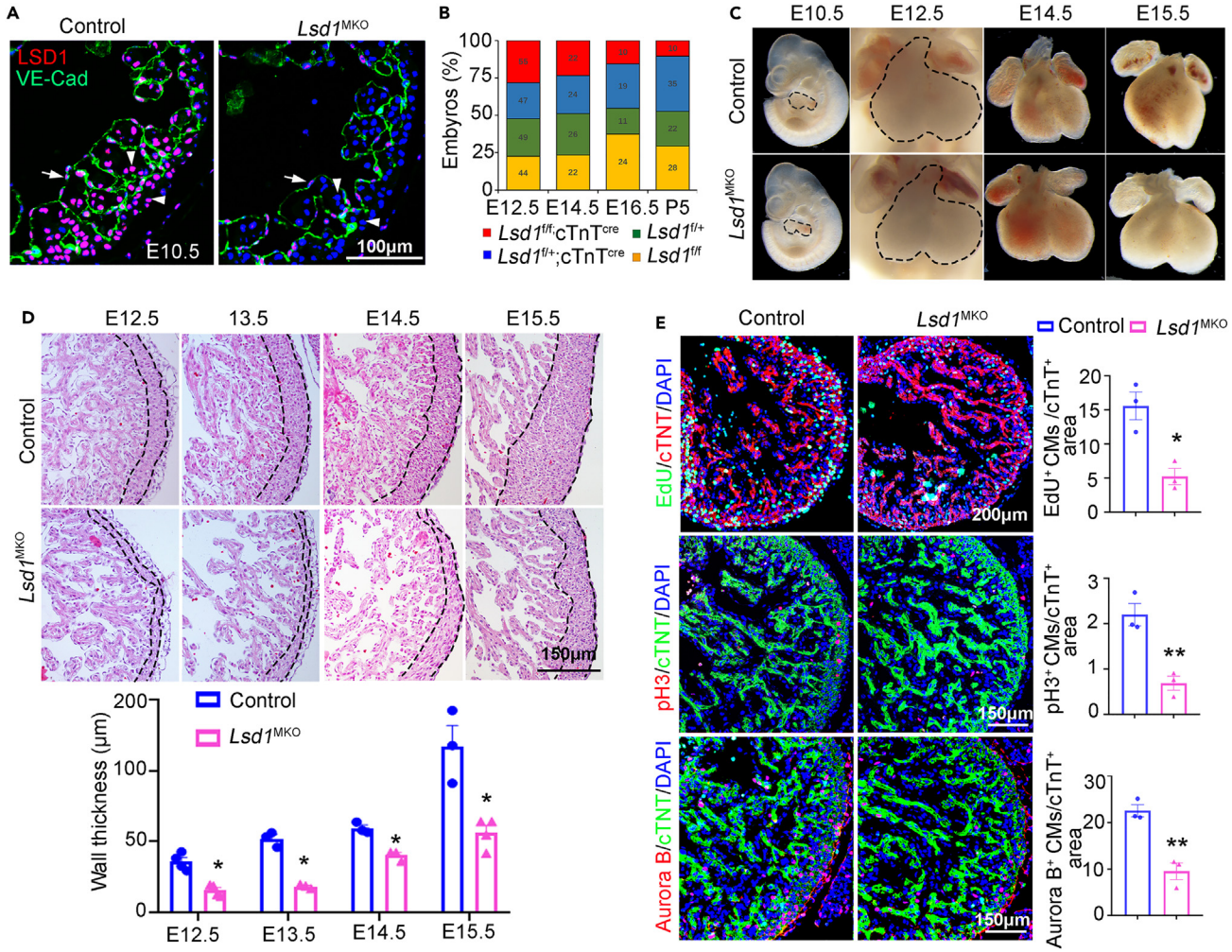

Figure 1. LSD1 is prerequisite for embryonic cardiomyocyte proliferation

(A) Immunostaining showing the LSD1 expression in the endocardium (arrows) and myocardium (arrowheads) in E10.5 control (*Lsd1*$^{f/f}$ or *Lsd1*$^{f/+}$) and *Lsd1*^{MKO} (*Lsd1*$^{f/f}$;*cTnT*^{Cre}) mouse embryos.

(B) A bar chart shows the embryo distribution from the crossing *Lsd1*$^{f/+}$;*cTnT*^{Cre} X *Lsd1*$^{f/f}$ at indicated stages.

(C) Gross views of control and *Lsd1*^{MKO} hearts.

(D) HE staining revealing the morphology of left ventricle; the compaction myocardium is outlined by the dashed lines. The thickness of compaction myocardium was quantified and presented in the bar chart. At least three embryos from each genotype were used for quantification.

(E) Immunostaining of EdU, pH3 and Aurora B revealing proliferating cells; cTNT co-staining marks the cardiomyocytes. The number of cells labeled with specific markers was quantified and presented as the ratio of cell numbers to cTNT^{+} area. The bar charts on the right showing the quantitative results for each staining. At least three embryos from each genotype were analyzed. (*) p value <0.05, (**) p value < 0.01 by unpaired Student's *t* test.

significantly augmented the level of *Cend1* (Figure 3F). Together, these results indicate that *Cend1* is negatively regulated by LSD1 in cardiomyocytes, which suggests that *Cend1* is a key LSD1 target regulating cardiomyocyte proliferation.

LSD1 is known to regulate gene transcription through removing H3K4me1/2 and H3K9me1/2 on histone 3.[16,17] Immunostaining showed increased levels of H3K4me1, H3K4me2 and H3K9me1, but decreased level of H3K9me2 in embryonic hearts of *Lsd1*^{MKO} embryos as compared with controls (Figures 3G and S5A). Because H3K4me1/2 and H3K9me1/2 are known to promote and repress gene transcription, respectively, we focused on H3K4me1/2. *Lsd1* deletion in neonatal cardiomyocytes significantly augmented the levels of H3K4me2 (Figure 3H). Consistent with these findings, the pharmacological inhibition of LSD1 augmented the levels of H3K4me1/2 in cultured primary cardiomyocytes and H9C2 cells (Figures 3I, S5B, and S5C), which suggests that this upregulation of H3K4me1/2 might contribute to the LSD1 suppression of *Cend1*. Chip-seq data from embryonic mouse hearts and human embryonic stem cells (Cistrome Data Browser) revealed the enrichment of H3K4me2 in the promoter of *Cend1* (Figure S5D). We used Chip-qPCR to confirm the enrichment of H3K4me2 in the *Cend1* promoter in H9C2 cells, which was further elevated by LSD1 inhibition (Figures 3J, S5E, and S5F). These results suggest that LSD1 suppresses the transcription of *Cend1* by erasing H3K4me2 marks at its promoter. Next, we performed luciferase reporter assays to test the

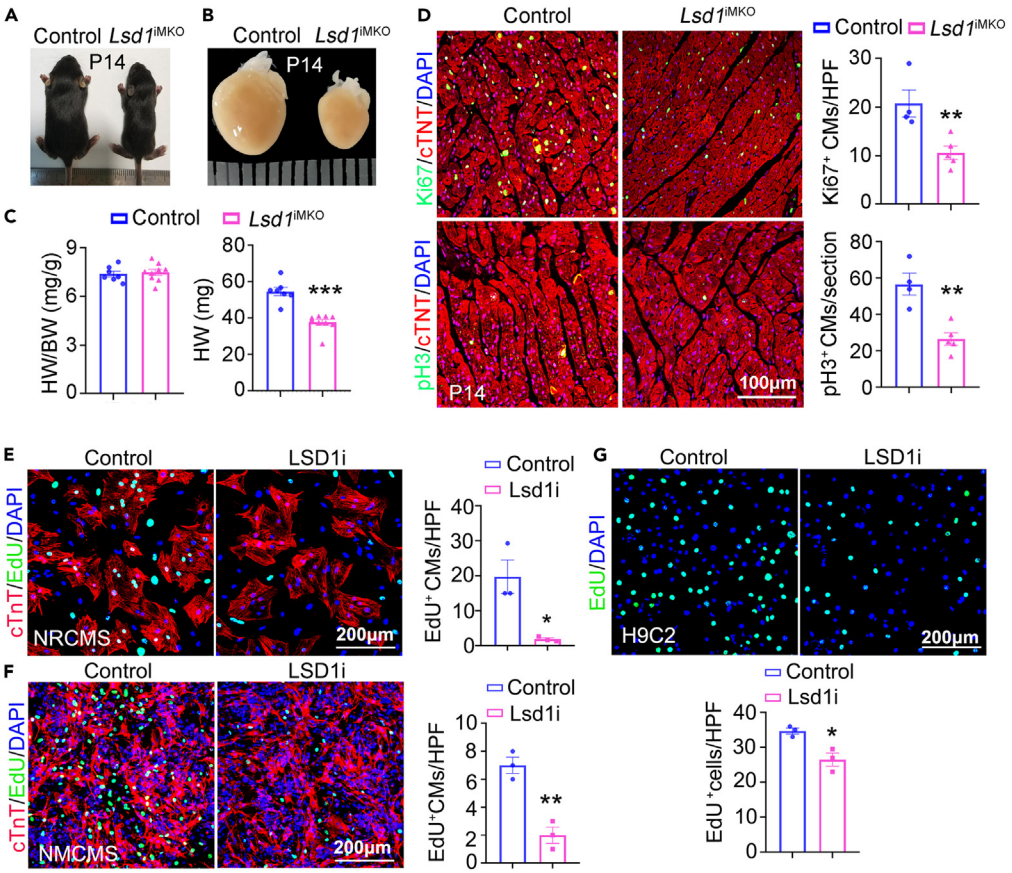

Figure 2. LSD1 is essential for neonatal cardiomyocyte proliferation

(A and B) The *Lsd1*$^{f/f}$ mice at postnatal day 1 (P1) were injected with AAV9-cTNTCre virus to induce the deletion of *Lsd1* in cardiomyocytes (*Lsd1*^{iMKO}); mice receiving control virus were used as controls. Representative images show the gross views of mice and hearts at P14.

(C) Ratio of heart to body weight, and heart weight. Control, n = 7. *Lsd1*^{iMKO}, n = 9.

(D) Immunostaining of Ki67 and pH3 indicating proliferating cells, and cTNT co-staining marking the cardiomyocytes. The bar charts showing the number of Ki67 and cTNT double-positive cells in each high power field (HPF) or pH3 and cTNT double-positive cells per section. Control, n = 4. *Lsd1*^{iMKO}, n = 5.

(E–G) Neonatal rat cardiomyocytes (NRCMs) and neonatal mouse cardiomyocytes (NMCMs) were treated with 250 nM of LSD1 inhibitor (LSD1i) GSKLSD1; cardiomyocyte cell line H9C2 was cultured in media with 500 nM of GSKLSD1 for 24 h. Cell proliferation were evaluated by EdU labeling. n = 3/group. The number of EdU and cTnT double-positive cells in each high power field was quantified. (*) p value <0.05, (**) p value < 0.01, (***) p value <0.001 by unpaired Student's *t* test.

effects of LSD1 on the transactivation of the *Cend1* promoter. A 1-Kb promoter of the murine *Cend1* gene strongly drove the luciferase reporter (Figure 3K). Inhibition and overexpression of LSD1 respectively augmented and repressed the transcription of the *Cend1* promoter (Figures 3L and 3M). Together, these findings demonstrate that LSD1 inhibits the expression of *Cend1* at the transcriptional level by erasing the active histone mark H3K4me2 at its promoter.

Lysine-specific demethylase 1 deletion activates the p53 pathway

LSD1 is known to repress the activity of p53 by the demethylation of p53 at K370.[31] In addition, CEND1 has been reported to arrest cell cycle by the induction of p53 in neuroblastoma cells.[30] Thus, we explored whether LSD1 promotes cardiomyocyte proliferation by suppressing p53 pathway. On immunostaining, *Lsd1* deletion in embryonic and neonatal cardiomyocytes activated p53 pathway, as shown by the increased expression of p53, p21 and Rb1 and decreased level of pRb1 at mRNA and protein levels (Figures 4A–4E). Consistent with these *in vivo* findings, LSD1 inhibition by GSKLSD1 activated p53 pathway in cultured cardiomyocytes (Figures 4F, 4G, and S6A). Together, these findings indicate that LSD1 negatively regulates the anti-proliferative pathway p53 in cardiomyocytes during heart development.

CEND1 inhibits cardiomyocyte proliferation

In mice, cardiomyocyte proliferation largely reduced at P7 when compared to P1 (Figure S1D). To explore whether CEND1 was involved in this reduction of cardiomyocyte proliferation, we examined the mRNA level of *Cend1* in P1 and P7 mouse hearts by qPCR. The expression of

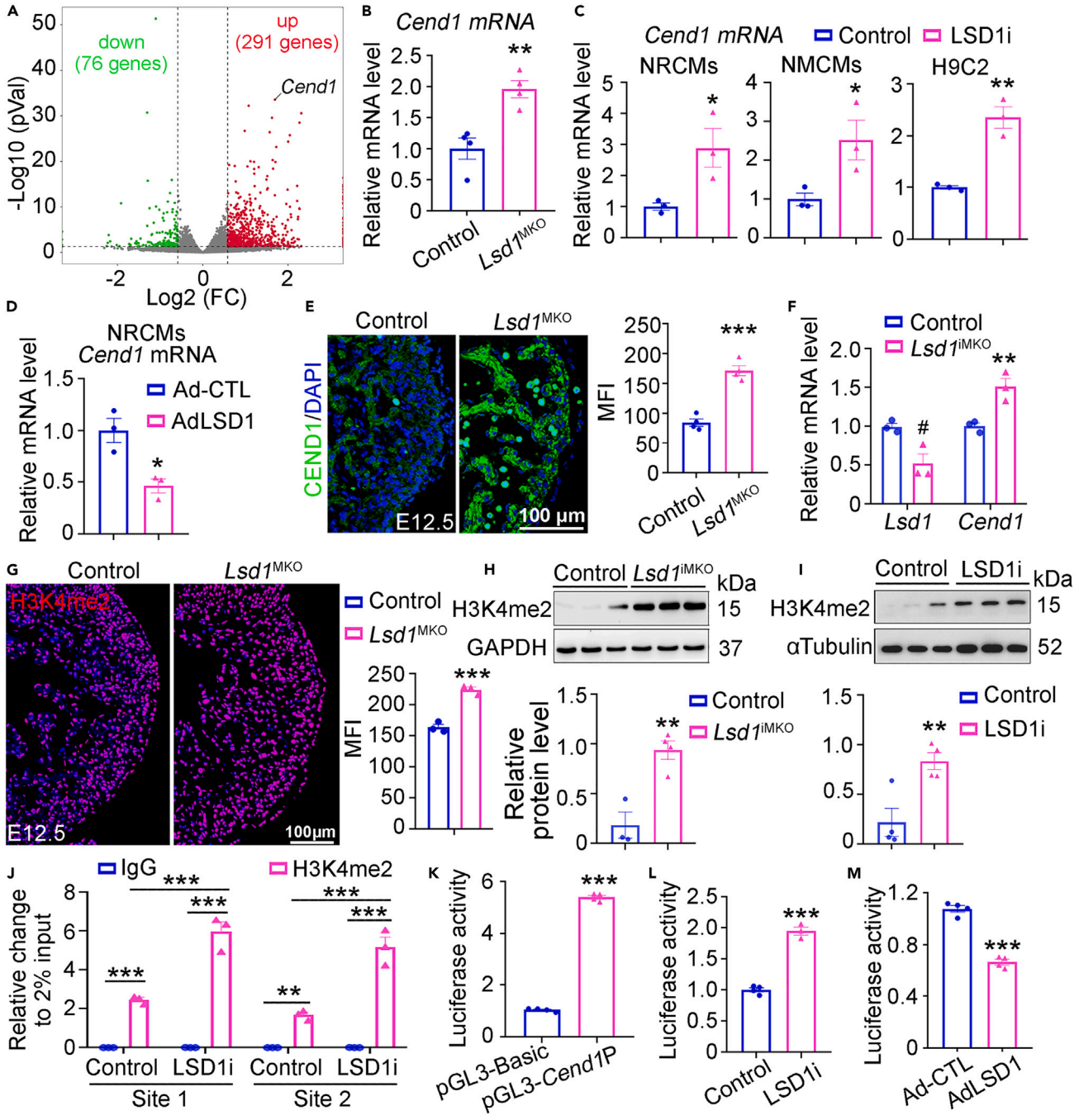

Figure 3. LSD1 represses *Cend1* expression by erasing H3K4me2 at its promoter

(A) Heart ventricle were isolated from E12.5 control and *Lsd1*^{MKO} embryos and subjected to RNA-seq analysis. Volcano plots show the differentially expressed genes.

(B–D) qPCR analysis of *Cend1* mRNA level in E12.5 hearts (B, n = 4/group), neonatal rat cardiomyocytes (NRCMs), neonatal mouse cardiomyocytes (NMCMs), and H9C2 cells. The cells were treated with LSD1 inhibitor GSKLSD1 (LSD1i). (C) n = 3/group. NRCMs were infected with AdLSD1 or Ad-CTL virus. (D) n = 3/group. The expression of *Cend1* was normalized to that of *Gapdh*.

(E) Immunostaining showing CEND1 expression in the left ventricle. The bar chart shows the mean fluorescence intensity (MFI) of the CEND1 signal. n = 4/group.

(F) qPCR analysis of *Lsd1* and *Cend1* mRNA level in the hearts of P7 control and *Lsd1*^{iMKO} mice. n = 3/group.

(G) immunostaining showing the expression of H3K4me2 in the left ventricle. The bar chart on right showing the MFI of indicated staining. n = 3/group.

(H and I) Western blot analysis of the levels of H3K4me2 in P14 hearts and NRCMs. n = 3–4/group.

Figure 3. *Continued*

(J) CHIP-qPCR analysis of H3K4me2 enrichment at the *Cend1* promoter in H9C2 cells. The cells were treated with GSKLSD1 to inhibit LSD1. n = 3/group. (K-M) A 1-kb murine *Cend1* promoter was cloned into pGl3-basic promoter and used for luciferase reporter assays in HEK293T cells. The promoter activities were analyzed with indicated treatments. n = 3–4/group. (*) p value <0.05, (**) p value < 0.01, (***) p value <0.001 by unpaired Student's *t* test or by One-way ANOVA with Tukey tests.

Cend1 in P7 hearts was significantly higher (Figure S7A), suggesting the upregulation of CEND1 might inhibit cardiomyocyte proliferation. Indeed, overexpression of CEND1 dramatically repressed the proliferation of NRCMs and upregulated the expression of p53 and p21 (Figures S7B and S7C).

Lysine-specific demethylase 1 promotes cardiomyocyte cell cycle by repressing CEND1

To explore whether LSD1 regulates cardiomyocyte cell cycle via the deduced CEND1 axis, we performed rescue experiments in neonatal rat cardiomyocytes. qPCR analysis confirmed that LSD1 inhibition significantly upregulated the expression of *Cend1*. However, this upregulation was abolished if *Cend1* was knockdown (Figure 5A). EdU labeling and pH3 immunostaining revealed that LSD1 inhibition reduced cardiomyocyte proliferation. This reduction was fully rescued by *Cend1* knockdown (Figure 5B). Similarly, LSD1 inhibition led to the cell-cycle arrest at G0/G1 phase, which could be relieved by *Cend1* knockdown (Figures 5C and 5D). As well, *Cend1* knockdown abolished p53 activation caused by LSD1 inhibition (Figure 5E), suggesting that LSD1 inhibition augmented p53 in a CEND1-dependent manner. In addition, this CEND1-dependent upregulation of p53 in the context of LSD1 inhibition was partially attenuated when the expression level of p53 was normalized to the number of G0/G1 cells (Figure S8). These results suggest that LSD1 promotes cardiomyocyte cell cycle via suppressing CEND1.

Cend1 deletion rectifies cardiomyocyte proliferation defect and embryonic lethality caused by lysine-specific demethylase 1 loss

To determine whether the LSD1-dependent suppression of *Cend1* is essential for cardiomyocyte proliferation *in vivo*, we crossed $Cend1^{-/-}$ mice with $Lsd1^{f/f}$ *and* $cTnT^{Cre}$ mice to establish the $Lsd1^{f/f}$;$Cend1^{-/-}$;$cTnT^{Cre}$ mouse line (hereafter refers to DKO) (Figure S9). Unlike the lethal phenotype found in $Lsd1^{MKO}$ embryos, DKO mice survived into adulthood (Figure 6A). The E12.5 DKO embryos had normal-sized hearts, but the hearts of $Lsd1^{MKO}$ embryos were much smaller than controls (Figure 6B). Similarly, the thin myocardial wall in $Lsd1^{MKO}$ embryos was corrected in DKO embryos (Figure 6C). Genetic deletion of *Cend1* also rescued the cardiomyocyte proliferation defect resulting from *Lsd1* loss (Figure 6D). Together, these results demonstrate that *Cend1* is a major downstream mediator involved in the LSD1-dependent regulation of cardiomyocyte proliferation during heart development.

Lysine-specific demethylase 1 regulates the cell cycle of human-induced pluripotent stem cell-derived cardiomyocytes by repressing CEND1

To demonstrate the translational relevance of our study, we explored the role of LSD1 in human-induced pluripotent stem cell-derived cardiomyocytes (hiPSC-CMs). In line with findings from mouse studies, LSD1 inhibition significantly augmented *CEND1* expression and activated the p53 pathway (Figures 7A and 7B). In addition, LSD1 inhibition suppressed cell proliferation and reduced cell cycle progression, which was restored by CRISPER-mediated *CEND1* knockout (Figures 7C and 7D). At molecular level, *CEND1* knockout attenuated the upregulation of p53 and p21 caused by LSD1 inhibition (Figure 7E). Together, these findings demonstrate that LSD1-CEND1 axis is a conserved mechanism of regulating human and mouse cardiomyocyte proliferation.

DISCUSSION

Cardiomyocyte proliferation is essential for the heart development and reactivation of adult cardiomyocyte proliferation represents an attractive approach for heart regeneration. However, the molecular mechanisms controlling cardiomyocyte cell cycle during development must be better understood to device an effective therapeutic strategy that unlocks the developmental paradigm in the adult heart. In the present study, using mouse models, primary cultured cardiomyocytes and hiPSC-CMs, we identified and characterized a LSD1-mediated epigenetic mechanism that critically regulates the progression of cardiomyocyte cell cycle in heart development. The mechanism behind involves that LSD1 inhibits p53 signaling likely through repressing *Cend1* by erasing the active histone mark H3K4me2 on its promoter (Figure 8).

Our work is the first to demonstrate that LSD1 promotes cardiomyocyte proliferation during embryonic and neonatal heart development. Mechanistically, we identified *Cend1* as a key downstream target suppressed by LSD1. *Cend1* is known to induces the cell cycle exit and promote cell differentiation, such as in neuronal progenitors.[30] In our study, *Cend1* knockdown reactivated the cell cycle progression in the cultured cardiomyocytes, which was initially suppressed by LSD1 inhibition. Furthermore, the genetic deletion of *Cend1* rescued the cardiomyocyte proliferation defect and embryonic lethal phenotype resulting from LSD1 deficiency. The rescue of ventricular wall thickness was significant but incomplete, suggesting that other targets besides *Cend1* may be involved in the LSD1-dependent regulation of myocardial growth. Indeed, several top upregulated genes by LSD1 loss are involved in the regulation of cell proliferation. For example, knockdown of *Tesc* has been shown to reduce p53 expression in human erythroleukemia (HEL) cells,[32] suggesting that *Tesc* might negatively regulate cell cycle. Transient receptor potential vanilloid 2 (Trpv2) has been demonstrated to negatively regulate glioma cell proliferation.[33,34] These

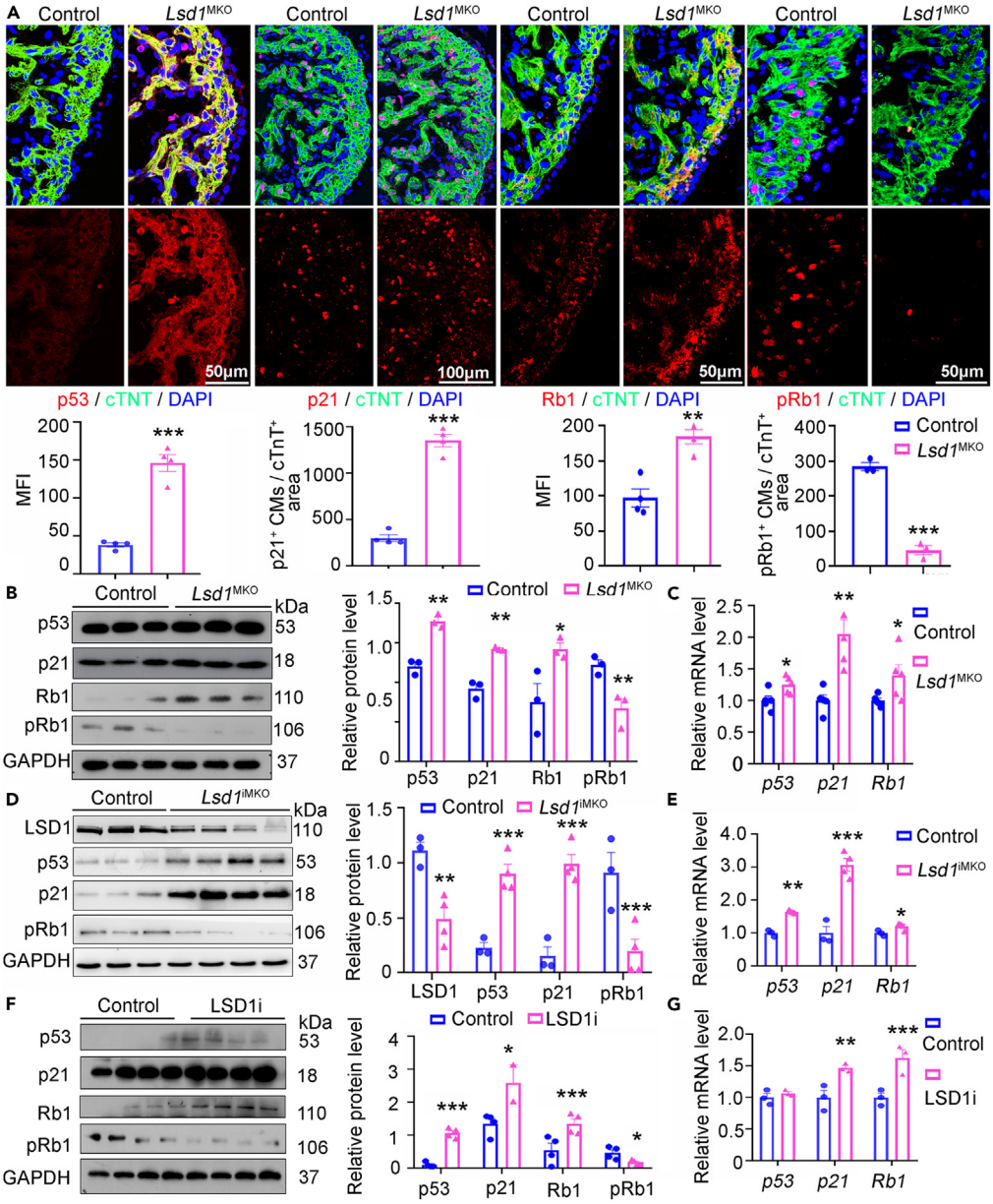

Figure 4. LSD1 loss augments p53 pathway

(A) Immunostaining showing the expression of p53, p21, Rb1 and pRb1 in the left ventricle of E12.5 hearts. The mean fluorescence intensity (MFI) of p53 and Rb1 staining was quantified. The number of cells labeled with p21 or pRb1 was quantified and presented as the ratio of cell numbers to $cTNT^{+}$ area. The bar charts show the quantitative results for indicated staining. n = 3–4/group.

(B) Western blot analysis of the protein level of p53, p21 and pRb1 in E12.5 control and $Lsd1^{MKO}$ hearts. n = 3/group.

(C) qPCR analysis of the mRNA levels of p53, p21 and Rb1 in E12.5 control and $Lsd1^{MKO}$ hearts. n = 4/group.

(D) Western blot analysis of the protein level of p53, p21, and pRb1 in P14 control and $Lsd1^{iMKO}$ hearts. n = 3–4/group.

(E) qPCR analysis of the mRNA levels of p53, p21 and Rb1 in P14 control and $Lsd1^{iMKO}$ hearts. n = 3–4/group.

(F and G) Western blot and qPCR was used to determine the protein (D) and mRNA (E) levels of p53, p21, and Rb1 in NRCMs treated with GSKLSD1. n = 3/group.

(*) p value <0.05, (**) p value < 0.01, (***) p value <0.001 by unpaired Student's *t* test.

observations suggest that the upregulation of *Tesc* and *Trpv2* might be also involved in the suppression of cardiomyocyte proliferation in *Lsd1* knockout embryos. Together, our findings suggest that *Cend1* is a major target of LSD1 and must be suppressed to support cardiomyocyte proliferation during normal heart development.

The cell cycle is controlled by both positive and negative regulators. As one of the critical factors negatively regulating cell proliferation, p21 inhibits CDK cyclins.[35] p21 is suppressed during heart development, because p21 upregulation severely impedes

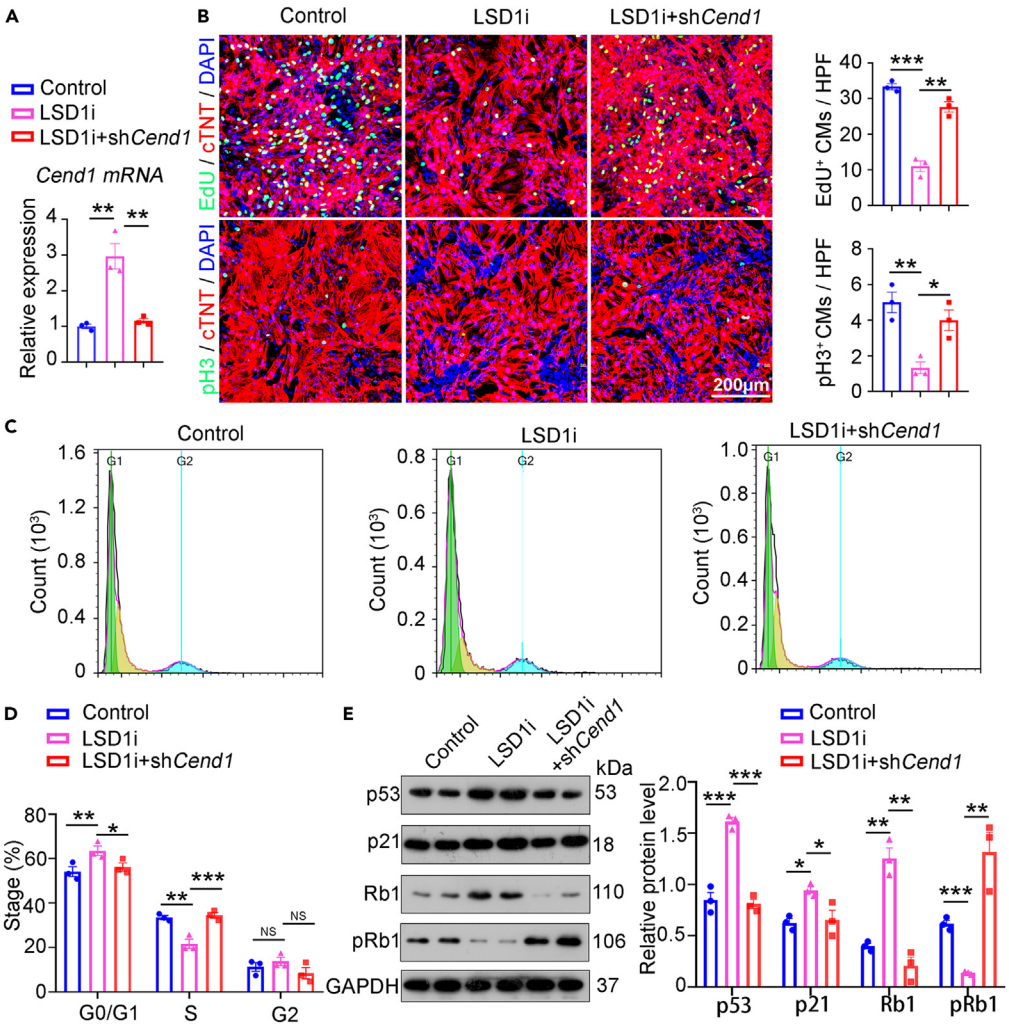

Figure 5. LSD1 promotes cardiomyocyte cell cycle via suppressing CEND1-p53 axis

(A) NRCMs were treated with LSD1 inhibitor GSKLSD1 and infected with lentivirus carrying sh*Cend1*. qPCR analysis of the mRNA level of *Cend1*. n = 3/group.

(B) EdU labeling and pH3 immunostaining revealing the proliferating NRCMs with indicated treatment. The bar charts showing the number of EdU/pH3 and cTNT double-positive cells in each high power field (HPF). n = 3/group.

(C and D) Flow cytometry analysis of the cell cycle of NRCMs under indicated conditions. Representative images show the distribution in cell cycle stages (C), while the bar chart showing the quantitative results (D) n = 3/group.

(E) Western blot analysis of the protein levels of p53, p21, Rb1, and pRb1 in NRCMs with indicated treatments. The bar chart showing the quantitative results. n = 4/group. (*) p value <0.05, (**) p value < 0.01, (***) p value <0.001 by One-way ANOVA with Tukey tests. NS, no significance.

cardiomyocyte proliferation and myocardial growth, leading to embryonic lethality.[36,37] p21 is known to be repressed by transcription factors GATA4[38] and MEIS1[10] during heart development. Here we identified that LSD1 is a new inhibitor of p21 during heart development. Multiple mechanisms are involved in p21 suppression, suggesting that p21 suppression is obligated to allow proper heart development.

Mechanistically, LSD1 regulates gene expression mainly through removing the H3K4me1/2 and H3K9me1/2 at the genome-wide scale.[39] We showed that *Cend1* promoter was marked by H3K4me2. Such modifications were augmented by LSD1 inhibitor GSKLSD1, which suggests that LSD1 may repress the transcription of *Cend1* by removing H3K4me2 at its promoter. We tested this idea by luciferase reporter assays and confirmed that LSD1 inhibition and overexpression augmented and reduced *Cend1* promoter activities, respectively. Similar to the prominent regulation of p53 by CEND1 in neural progenitor cell proliferation,[30] our findings suggest that LSD1 may negatively regulate p53 pathway via suppressing CEND1 in cardiomyocytes. LSD1 can demethylate p53 at K370 and regulate its activity in U2OS cells.[31] Whether this mechanism is also presented in cardiomyocyte was not investigated in this study and warrants further investigations. Hence, the LSD1-CEND1 axis is a new mechanism that suppresses p53 pathway to support cardiomyocyte proliferation for normal heart development. Interestingly, the deletion of

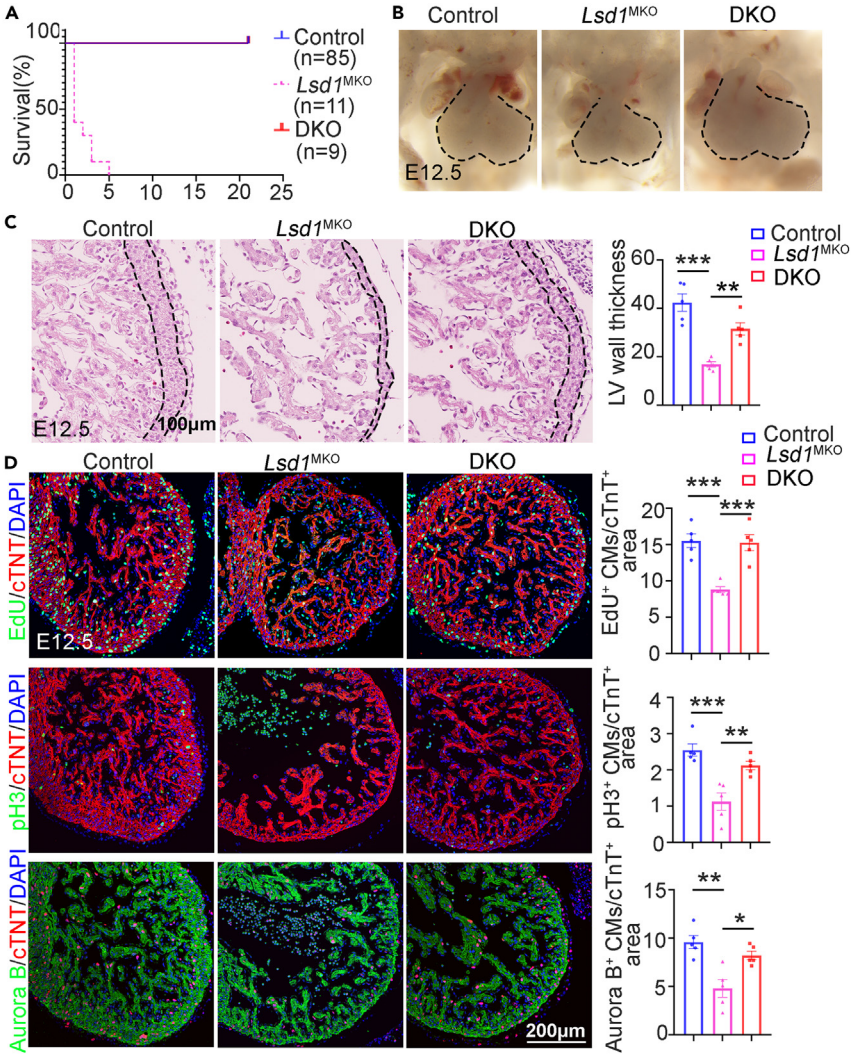

Figure 6. *Cend1* deletion rescues the cardiomyocyte proliferation defect and embryonic lethality caused by LSD1 loss

(A) survival curve.

(B) Gross views of hearts from control, *Lsd1*^{MKO} and DKO (*Lsd1*$^{f/f}$;*cTnT*^{Cre};*Cend1*$^{-/-}$) embryos.

(C) HE staining showing the morphology of left ventricle. The compaction myocardium is outlined by the dashed lines. The thickness of compaction myocardium was quantified and shown in the bar chart. n = 5/group.

(D) Immunostaining of EdU, pH3 and Aurora B revealing proliferating cells; cTNT co-staining marks the cardiomyocytes. The number of cells labeled with specific markers was quantified and presented as the ratio of cell numbers to cTNT^{+} area. The bar charts on the right showing the quantification for each staining. n = 5/group. (*) p value <0.05, (**) p value < 0.01, (***) p value <0.001 by One-way ANOVA with Tukey tests.

Rcor2, a co-repressor of LSD1, inhibits neural progenitor cell proliferation,[40] suggesting a potential role of LSD1-CEND1-p53 axis in regulation of neuronal development. However, this speculation needs to be validated experimentally. We showed that LSD1 inhibition resulted in cell-cycle arrest accompanying increased expression of CEND1 and p53, whereas CEND1 knockdown blocked the upregulation of p53. This finding suggests that LSD1 inhibition may upregulate p53 via CEND1. It is worth mentioning that this CEND1-dependent upregulation of p53 in the context of LSD1 inhibition appeared cell cycle dependent, as when we normalized the expression level of p53 to the number of G0/G1 cells, such upregulation was partially attenuated (Figure S8). Thus, CEND1 likely regulates p53 expression indirectly via cell cycle suppression, as p53 is known to be regulated in a cell cycle dependent manner.[41] Future studies are needed to confirm the direct regulation of p53 by CEND1 in cardiomyocytes and to decipher the underlying mechanisms.

In summary, our findings identify that the LSD1-CEND1 axis is an essential mechanism epigenetically controlling cardiomyocyte proliferation during mouse heart development. We also demonstrate the essentiality of LSD1-CEND1 axis in the regulation of the cell cycle of hiPSC-CMs, which informs the translational meaning of this novel regulatory axis. Future studies may focus on exploring whether the activation of LSD1 could promote heart regeneration following myocardial infraction in adult mice.

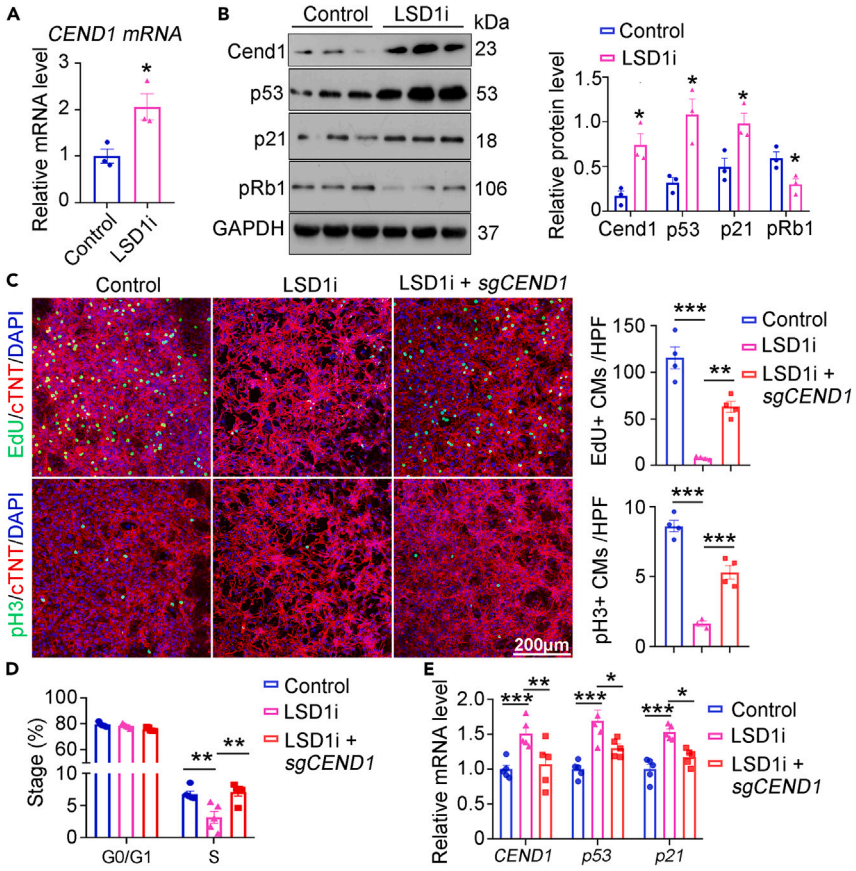

Figure 7. LSD1 promotes cell cycle via suppressing CEND1 in hiPSC-CMs

Human-induced pluripotent stem cell-derived cardiomyocytes (hiPSC-CMs) were used to study the role of LSD1-CEND1-p53 axis in the regulation of cell cycle and proliferation.

(A) qPCR analysis of the *CEND1* mRNA level in hiPSC-CMs treated with 1 mM of GSKLSD1 (LSD1i) or vehicle as controls. The expression of CEND1 was normalized to that of GAPDH. n = 3/group.

(B) Western blot analysis of the protein level of CEND1, p53, P21, and pRb1. n = 3/group.

(C) EdU labeling and pH3 immunostaining revealing the proliferation of hiPSC-CMs treated with GSKLSD1 or lentivirus carrying CRISPER against *CEND1*. n = 4/group. The proliferation of cardiomyocytes was quantified by the number of cells labeled by EdU/pH3 and cTnT per high power field.

(D) Flow cytometry results of the cell cycle of hiPSC-CMs under indicated conditions. n = 5/group.

(E) qPCR analysis of the mRNA level of *CEND1*, *p53*, and *p21* in hiPSC-CMs with indicated treatments. The expression of target genes was normalized to that of *GAPDH*. n = 5/group. (*) p value <0.05, (**) p value < 0.01, (***) p value <0.001 by unpaired Student's *t* test or by One-way ANOVA with Tukey tests. HPF, high power field.

Limitations of the study

Genetic deletion of *Cend1* rescued cardiomyocyte proliferation defect and embryonic lethality in *Lsd1* null embryos, indicating that *Cend1* is a major target suppressed by LSD1 during murine heart development. However, this rescue was not a full recovery, suggesting that there must be other mediators which were not investigated in the present study. In addition, the mechanism through which CEND1 regulates p53 pathway were not explored and warrants further investigations in future studies.

STAR★METHODS

Detailed methods are provided in the online version of this paper and include the following:

- KEY RESOURCES TABLE
- RESOURCE AVAILABILITY
  - Lead contact
  - Materials availability
  - Data and code availability

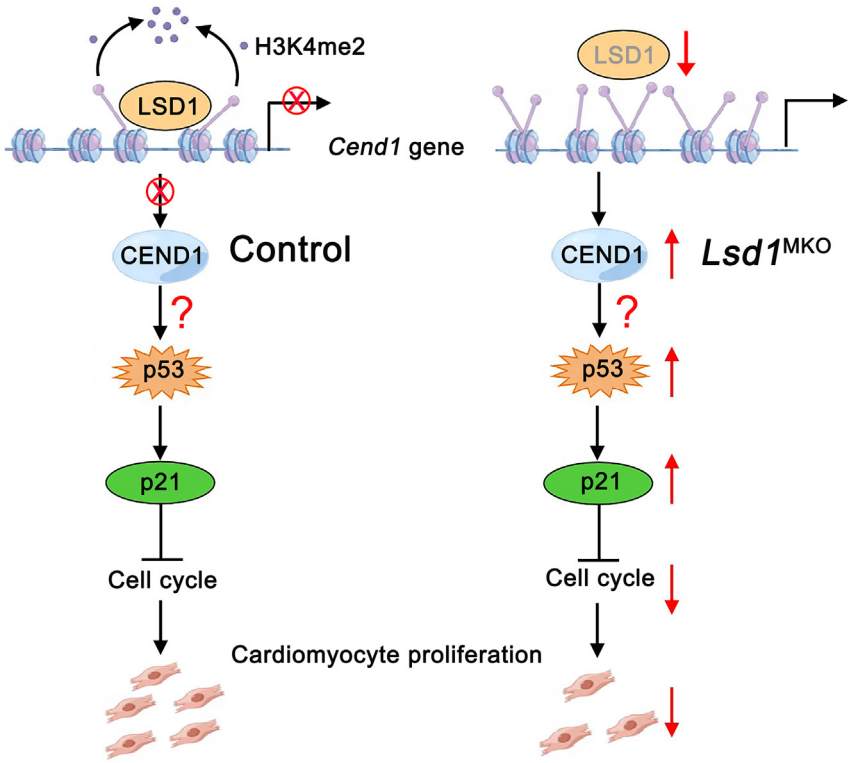

Figure 8. Working model of the LSD1-CEND1 axis regulation of cardiomyocyte proliferation

In controls, LSD1 removes the active histone mark H3K4me2 at *Cend1* promoter, thus suppressing *Cend1* transcription and reducing CEND1 expression. CEND1 may positively regulate the p53 signaling pathway, which inhibits cardiomyocyte proliferation by repressing cell cycle. In *Lsd1*^{MKO}, LSD1 loss increases the level of H3K4me2 at *Cend1* promoter, thus elevating CEND1 expression. The increased CEND1 expression inhibits cell cycle and cardiomyocyte proliferation potentially through augmenting p53 pathway.

SUPPLEMENTAL INFORMATION

Supplemental information can be found online at https://doi.org/10.1016/j.isci.2023.108722.

ACKNOWLEDGMENTS

This work was supported by the National Key R&D Program of China (2019YFA0802300, to Y.W.; 2021YFA1301200 to Z.Y.), the National Natural Science Foundation of China (81970266, to Y.W.; 92049203 to Z.Y., 81970257 to D.Z.), Department of Human and Social Affairs of Shaanxi Province in China (2019001, to Y.W.). We gratefully acknowledge Dr. Maoqing Ye at Fudan University for critical technical supports.

AUTHOR CONTRIBUTIONS

H.L., Y.W., and Z.Y. conceived the concept. H.L., R.Z., and S.L. designed and conducted most of the experiments. Y.L. analyzed the RNA-seq data. J.D., Y.F., H.S., B.L., and L.L. collected samples and performed histological analyses. H.L., Y.W., R.Z., S.L., and D.Z. analyzed the data. Y.W., Z.Y., J.S., and Y.Z. supervised the project. H.L., Y.W., J.S., and B.Z. wrote the article with feedback from all authors. Y.W., Z.Y., and D.Z. provided grant supports.

DECLARATION OF INTERESTS

The authors declare no competing interests.

Received: June 30, 2023
Revised: September 29, 2023
Accepted: December 11, 2023
Published: December 13, 2023

REFERENCES

1. Bergmann, O., Zdunek, S., Felker, A., Salehpour, M., Alkass, K., Bernard, S., Sjostrom, S.L., Szewczykowska, M., Jackowska, T., Dos Remedios, C., et al. (2015). Dynamics of Cell Generation and Turnover in the Human Heart. Cell *161*, 1566–1575.
2. Kikuchi, K., Holdway, J.E., Werdich, A.A., Anderson, R.M., Fang, Y., Egnaczyk, G.F., Evans, T., Macrae, C.A., Stainier, D.Y.R., and Poss, K.D. (2010). Primary contribution to zebrafish heart regeneration by gata4(+) cardiomyocytes. Nature *464*, 601–605.
3. Xiang, F.-L., Guo, M., and Yutzey, K.E. (2016). Overexpression of Tbx20 in Adult Cardiomyocytes Promotes Proliferation and Improves Cardiac Function After Myocardial Infarction. Circulation *133*, 1081–1092.
4. Xiao, C., Gao, L., Hou, Y., Xu, C., Chang, N., Wang, F., Hu, K., He, A., Luo, Y., Wang, J., et al. (2016). Chromatin-remodelling factor Brg1 regulates myocardial proliferation and regeneration in zebrafish. Nat. Commun. *7*, 13787.
5. Xin, M., Kim, Y., Sutherland, L.B., Murakami, M., Qi, X., McAnally, J., Porrello, E.R., Mahmoud, A.I., Tan, W., Shelton, J.M., et al. (2013). Hippo pathway effector Yap promotes cardiac regeneration. Proc. Natl. Acad. Sci. USA *110*, 13839–13844.
6. Heallen, T., Zhang, M., Wang, J., Bonilla-Claudio, M., Klysik, E., Johnson, R.L., and Martin, J.F. (2011). Hippo pathway inhibits Wnt signaling to restrain cardiomyocyte proliferation and heart size. Science (New York, N.Y.) *332*, 458–461.
7. Li, Y., Feng, J., Song, S., Li, H., Yang, H., Zhou, B., Li, Y., Yue, Z., Lian, H., Liu, L., et al. (2020). gp130 Controls Cardiomyocyte Proliferation and Heart Regeneration. Circulation *142*, 967–982.
8. D'Uva, G., Aharonov, A., Lauriola, M., Kain, D., Yahalom-Ronen, Y., Carvalho, S., Weisinger, K., Bassat, E., Rajchman, D., Yifa, O., et al. (2015). ERBB2 triggers mammalian heart regeneration by promoting cardiomyocyte dedifferentiation and proliferation. Nat. Cell Biol. *17*, 627–638.
9. Tao, G., Kahr, P.C., Morikawa, Y., Zhang, M., Rahmani, M., Heallen, T.R., Li, L., Sun, Z., Olson, E.N., Amendt, B.A., and Martin, J.F. (2016). Pitx2 promotes heart repair by activating the antioxidant response after cardiac injury. Nature *534*, 119–123.
10. Mahmoud, A.I., Kocabas, F., Muralidhar, S.A., Kimura, W., Koura, A.S., Thet, S., Porrello, E.R., and Sadek, H.A. (2013). Meis1 regulates postnatal cardiomyocyte cell cycle arrest. Nature *497*, 249–253.
11. Bassat, E., Mutlak, Y.E., Genzelinakh, A., Shadrin, I.Y., Baruch Umansky, K., Yifa, O., Kain, D., Rajchman, D., Leach, J., Riabov Bassat, D., et al. (2017). The extracellular matrix protein agrin promotes heart regeneration in mice. Nature *547*, 179–184.
12. Wu, Y., Zhou, L., Liu, H., Duan, R., Zhou, H., Zhang, F., He, X., Lu, D., Xiong, K., Xiong, M., et al. (2021). LRP6 downregulation promotes cardiomyocyte proliferation and heart regeneration. Cell Res. *31*, 450–462.
13. Quaife-Ryan, G.A., Sim, C.B., Ziemann, M., Kaspi, A., Rafehi, H., Ramialison, M., El-Osta, A., Hudson, J.E., and Porrello, E.R. (2017). Multicellular Transcriptional Analysis of Mammalian Heart Regeneration. Circulation *136*, 1123–1139.
14. Sdek, P., Zhao, P., Wang, Y., Huang, C.J., Ko, C.Y., Butler, P.C., Weiss, J.N., and Maclellan, W.R. (2011). Rb and p130 control cell cycle gene silencing to maintain the postmitotic phenotype in cardiac myocytes. J. Cell Biol. *194*, 407–423.
15. Hille, S., Dierck, F., Kühl, C., Sosna, J., Adam-Klages, S., Adam, D., Lüllmann-Rauch, R., Frey, N., and Kuhn, C. (2016). Dyrk1a regulates the cardiomyocyte cell cycle via D-cyclin-dependent Rb/E2f-signalling. Cardiovasc. Res. *110*, 381–394.
16. Shi, Y., Lan, F., Matson, C., Mulligan, P., Whetstine, J.R., Cole, P.A., Casero, R.A., and Shi, Y. (2004). Histone demethylation mediated by the nuclear amine oxidase homolog LSD1. Cell *119*, 941–953.
17. Metzger, E., Wissmann, M., Yin, N., Müller, J.M., Schneider, R., Peters, A.H.F.M., Günther, T., Buettner, R., and Schüle, R. (2005). LSD1 demethylates repressive histone marks to promote androgen-receptor-dependent transcription. Nature *437*, 436–439.
18. Lim, S., Janzer, A., Becker, A., Zimmer, A., Schüle, R., Buettner, R., and Kirfel, J. (2010). Lysine-specific demethylase 1 (LSD1) is highly expressed in ER-negative breast cancers and a biomarker predicting aggressive biology. Carcinogenesis *31*, 512–520.
19. Liu, C., Liu, L., Chen, X., Cheng, J., Zhang, H., Zhang, C., Shan, J., Shen, J., and Qian, C. (2018). LSD1 Stimulates Cancer-Associated Fibroblasts to Drive Notch3-Dependent Self-Renewal of Liver Cancer Stem-like Cells. Cancer Res. *78*, 938–949.
20. Leiendecker, L., Jung, P.S., Krecioch, I., Neumann, T., Schleiffer, A., Mechtler, K., Wiesner, T., and Obenauf, A.C. (2020). LSD1 inhibition induces differentiation and cell death in Merkel cell carcinoma. EMBO Mol. Med. *12*, e12525.
21. Shen, D.-D., Pang, J.-R., Bi, Y.-P., Zhao, L.-F., Li, Y.-R., Zhao, L.-J., Gao, Y., Wang, B., Wang, N., Wei, L., et al. (2022). LSD1 deletion decreases exosomal PD-L1 and restores T-cell response in gastric cancer. Mol. Cancer *21*, 75.
22. Zhang, W., Ruan, X., Li, Y., Zhi, J., Hu, L., Hou, X., Shi, X., Wang, X., Wang, J., Ma, W., et al. (2022). KDM1A promotes thyroid cancer progression and maintains stemness through the Wnt/β-catenin signaling pathway. Theranostics *12*, 1500–1517.
23. Lee, C., Rudneva, V.A., Erkek, S., Zapatka, M., Chau, L.Q., Tacheva-Grigorova, S.K., Garancher, A., Rusert, J.M., Aksoy, O., Lea, R., et al. (2019). Lsd1 as a therapeutic target in Gfi1-activated medulloblastoma. Nat. Commun. *10*, 332.
24. Takagi, S., Ishikawa, Y., Mizutani, A., Iwasaki, S., Matsumoto, S., Kamada, Y., Nomura, T., and Nakamura, K. (2017). LSD1 Inhibitor T-3775440 Inhibits SCLC Cell Proliferation by Disrupting LSD1 Interactions with SNAG Domain Proteins INSM1 and GFI1B. Cancer Res. *77*, 4652–4662.
25. Wang, J., Scully, K., Zhu, X., Cai, L., Zhang, J., Prefontaine, G.G., Krones, A., Ohgi, K.A., Zhu, P., Garcia-Bassets, I., et al. (2007). Opposing LSD1 complexes function in developmental gene activation and repression programmes. Nature *446*, 882–887.
26. Nicholson, T.B., Singh, A.K., Su, H., Hevi, S., Wang, J., Bajko, J., Li, M., Valdez, R., Goetschkes, M., Capodieci, P., et al. (2013). A hypomorphic lsd1 allele results in heart development defects in mice. PLoS One *8*, e60913.
27. Zhou, Z.G., Chen, J.B., Zhang, R.X., Ye, L., Wang, J.C., Pan, Y.X., Wang, X.H., Li, W.X., Zhang, Y.J., Xu, L., and Chen, M.S. (2020). Tescalcin is an unfavorable prognosis factor that regulats cell proliferation and survival in hepatocellular carcinoma patients. Cancer Commun. *40*, 355–369.
28. Soh, Y.Q.S., Mikedis, M.M., Kojima, M., Godfrey, A.K., de Rooij, D.G., and Page, D.C. (2017). Meioc maintains an extended meiotic prophase I in mice. PLoS Genet. *13*, e1006704.

29. Zhang, W., He, X., Yin, H., Cao, W., Lin, T., Chen, W., Diao, W., Ding, M., Hu, H., Mo, W., et al. (2022). Allosteric activation of the metabolic enzyme GPD1 inhibits bladder cancer growth via the lysoPC-PAFR-TRPV2 axis. J. Hematol. Oncol. *15*, 93.
30. Georgopoulou, N., Hurel, C., Politis, P.K., Gaitanou, M., Matsas, R., and Thomaidou, D. (2006). BM88 is a dual function molecule inducing cell cycle exit and neuronal differentiation of neuroblastoma cells via cyclin D1 down-regulation and retinoblastoma protein hypophosphorylation. J. Biol. Chem. *281*, 33606–33620.
31. Huang, J., Sengupta, R., Espejo, A.B., Lee, M.G., Dorsey, J.A., Richter, M., Opravil, S., Shiekhattar, R., Bedford, M.T., Jenuwein, T., and Berger, S.L. (2007). p53 is regulated by the lysine demethylase LSD1. Nature *449*, 105–108.
32. Levay, K., and Slepak, V.Z. (2014). Regulation of Cop9 signalosome activity by the EF-hand Ca2+-binding protein tescalcin. J. Cell Sci. *127*, 2448–2459.
33. Nabissi, M., Morelli, M.B., Amantini, C., Farfariello, V., Ricci-Vitiani, L., Caprodossi, S., Arcella, A., Santoni, M., Giangaspero, F., De Maria, R., and Santoni, G. (2010). TRPV2 channel negatively controls glioma cell proliferation and resistance to Fas-induced apoptosis in ERK-dependent manner. Carcinogenesis *31*, 794–803.
34. Morelli, M.B., Nabissi, M., Amantini, C., Farfariello, V., Ricci-Vitiani, L., di Martino, S., Pallini, R., Larocca, L.M., Caprodossi, S., Santoni, M., et al. (2012). The transient receptor potential vanilloid-2 cation channel impairs glioblastoma stem-like cell proliferation and promotes differentiation. Int. J. Cancer *131*, E1067–E1077.
35. Engeland, K. (2022). Cell cycle regulation: p53-p21-RB signaling. Cell Death Differ. *29*, 946–960.
36. Pasumarthi, K.B.S., and Field, L.J. (2002). Cardiomyocyte cell cycle regulation. Circ. Res. *90*, 1044–1054.
37. Poolman, R.A., Gilchrist, R., and Brooks, G. (1998). Cell cycle profiles and expressions of p21CIP1 AND P27KIP1 during myocyte development. Int. J. Cardiol. *67*, 133–142.
38. Singh, M.K., Li, Y., Li, S., Cobb, R.M., Zhou, D., Lu, M.M., Epstein, J.A., Morrisey, E.E., and Gruber, P.J. (2010). Gata4 and Gata5 cooperatively regulate cardiac myocyte proliferation in mice. J. Biol. Chem. *285*, 1765–1772.
39. Perillo, B., Tramontano, A., Pezone, A., and Migliaccio, A. (2020). LSD1: more than demethylation of histone lysine residues. Exp. Mol. Med. *52*, 1936–1947.
40. Wang, Y., Wu, Q., Yang, P., Wang, C., Liu, J., Ding, W., Liu, W., Bai, Y., Yang, Y., Wang, H., et al. (2016). LSD1 co-repressor Rcor2 orchestrates neurogenesis in the developing mouse brain. Nat. Commun. *7*, 10481.
41. Fogal, V., Hsieh, J.K., Royer, C., Zhong, S., and Lu, X. (2005). Cell cycle-dependent nuclear retention of p53 by E2F1 requires phosphorylation of p53 at Ser315. EMBO J. *24*, 2768–2782.
42. Kerenyi, M.A., Shao, Z., Hsu, Y.-J., Guo, G., Luc, S., O'Brien, K., Fujiwara, Y., Peng, C., Nguyen, M., and Orkin, S.H. (2013). Histone demethylase Lsd1 represses hematopoietic stem and progenitor cell signatures during blood cell maturation. Elife *2*, e00633.
43. Wu, B., Zhou, B., Wang, Y., Cheng, H.-L., Hang, C.T., Pu, W.T., Chang, C.-P., and Zhou, B. (2010). Inducible cardiomyocyte-specific gene disruption directed by the rat Tnnt2 promoter in the mouse. Genesis *48*, 63–72.
44. Chen, S., Zhou, Y., Chen, Y., and Gu, J. (2018). fastp: an ultra-fast all-in-one FASTQ preprocessor. Bioinformatics *34*, i884–i890.
45. Kim, D., Paggi, J.M., Park, C., Bennett, C., and Salzberg, S.L. (2019). Graph-based genome alignment and genotyping with HISAT2 and HISAT-genotype. Nat. Biotechnol. *37*, 907–915.
46. Liao, Y., Smyth, G.K., and Shi, W. (2014). featureCounts: an efficient general purpose program for assigning sequence reads to genomic features. Bioinformatics *30*, 923–930.
47. Love, M.I., Huber, W., and Anders, S. (2014). Moderated estimation of fold change and dispersion for RNA-seq data with DESeq2. Genome Biol. *15*, 550.
48. Yu, G., Wang, L.G., Han, Y., and He, Q.Y. (2012). clusterProfiler: an R package for comparing biological themes among gene clusters. OMICS *16*, 284–287.

STAR★METHODS

KEY RESOURCES TABLE

REAGENT or RESOURCE	SOURCE	IDENTIFIER
Antibodies		
antibodies	see Table S2	NA
Chemicals, peptides, and recombinant proteins		
GSKLSD1	Sigma	Cat# SML1072
EdU Kit	Invitrogen	Cat# A10044
DeadEnd Fluorometric TUNEL System	Promega	Cat# G3250
Pierce BCA Protein Assay Kit	Thermo	Cat# 23225
Luciferase Assay System with Reporter Lysis Buffer	Promega	Cat# E4030
SimpleChIP Enzymatic Chromatin IP Kit	CST	Cat# 9003
Deposited data		
RNAseq	GEO database	GSE244414
Oligonucleotides		
qPCR primers	see Table S1	NA
Software and algorithms		
GraphPad Prism 8.0.1	GraphPad Software	https://www.graphpad.com/
R 4.2.1	R Project	https://www.r-project.org/
ImageJ	NIH	https://imagej.net/
Adobe Photoshop CC 2019	Adobe	https://www.adobe.com/

RESOURCE AVAILABILITY

Lead contact

Further information and requests for resources and reagents should be directed to and will be fulfilled by the lead contact, Yidong Wang (yidwang119@xjtu.edu.cn).

Materials availability

This study did not generate new unique reagents.

Data and code availability

- The data supporting the findings of this study are available within the article and its Supplemental Material. Complete RNA-seq data set has been deposited in the Gene Expression Omnibus database and are publicly available. Accession number is listed in the key resources table.
- This paper does not report any original code.
- Any additional information required to reanalyze the data reported in this paper is available from the lead contact upon request.

EXPERIMENTAL MODEL AND STUDY PARTICIPANT DETAILS

Animals

Cardiomyocyte-specific *Lsd1* knockout mice (*Lsd1*^{MKO}) were generated by crossing *Lsd1*$^{f/f}$ mice[42] with *cTnT*^{cre} mice.[43] Inducible cardiomyocyte-specific *Lsd1* knockout mice (*Lsd1*^{iMKO}) were obtained by injection of AAV9-*cTnT*^{cre} (10 μl per pup) into left ventricle of postnatal day 1 (P1) *Lsd1*$^{f/f}$ mice. The *Lsd1*$^{f/f}$ mice were crossed with *cTnT*^{cre} and *Cend1*$^{-/-}$ mice to generate *Lsd1* and *Cend1* double knockout mice (DKO) (Figure S9). *Cend1*$^{-/-}$ mice were purchased from GemPharmatech Co., Ltd. All animals were feed in a 12-h light/dark cycle in a temperature-controlled room in the Animal Research Center of Xian Jiaotong University. Noontime on the day of detecting vaginal plugs was designated as embryonic day (E) 0.5. The mice at postnatal day 14 and embryos (between E12.5 and E16.5) were used for experiments. The mice were euthanized by inhalation of carbon dioxide gas using a euthanasia chamber. All animal experiments conformed to the Guidelines for Care and Use of Laboratory Animals published by the National Institution of Health and were approved by the Institutional Animal Care and Use Committee (IACUC) of Xian Jiaotong University.

METHOD DETAILS

Histology and immunostaining

Hearts were collected, fixed in 4% paraformaldehyde (PFA) for 24 h, rinsed in PBS, dehydrated in a serial of gradient alcohol, dewaxed in xylene, embedded in paraffin, and sectioned at 5 μm thickness. Hematoxylin and Eosin (H&E) and Masson's trichrome staining were carried out to visualize the heart histology and fibrosis, respectively, according to the standard protocols. In addition, paraffin sections were immunostained for specific antibodies (Table S1). In brief, the tissues were rehydrated in a serial of ethanol and boiled two times in sodium citrate (Sigma, S1804) buffer (pH=6.0) or Tris-EDTA (pH = 9.0) for 10 min/time. The tissues were then blocked with 5% horse serum (Solaribo, SL042) for 1 h at room temperature and incubated with primary antibodies overnight at 4°C. After three washes with PBST, the tissue were incubated with secondary antibodies conjugated with fluorescence dyes (Table S1), then stained with DAPI (Beyotime, C1006) for 5 min, and images were acquired using a confocal microscope (Olympus FV3000, Core Facilities Sharing Platform of School of Basic Medical Sciences).

Cell proliferation and apoptosis assays

The pregnant and neonatal mice was intraperitoneally injected with 5-ethynyl-2′-deoxyuridine (EdU, 100 mg/kg) 2 h prior to the collection of hearts. The isolated hearts were processed for paraffin sections and subjected to and antibody and EdU staining (Click-iT® EdU Alexa Fluor® 488 Imaging Kit, Life Technologies); the cell nucleus was counterstained with DAPI (Vector labs). To label the proliferating cardiomyocytes, 20 μM EDU was added into the medium 2 h prior to sample collection. The cells were fixed in 4% PFA for 15 min, washed with PBS, permeated using PBS containing 0.05% Triton, blocked with 5% BSA (Millipore, FC0077), then underwent antibody and EDU staining as described above. Apoptotic cells were detected by using a TUNEL kit (Premaga, G3250). Images were collected using a confocal microscope and analyzed by using Image J.

Quantification of immunostaining

The quantification of immunostaining was performed in Image J. The number of cells labeled with specific markers (EdU, pH3, Aurora B, Ki67, p21, and pRb1) was quantified. The cTNT staining was used for specific quantification of cardiomyocyte. The data was presented as the following ways: (1) the ratio of cell numbers to cTNT+ area; (2) the cell numbers per high power field (HPF); (3) the cell numbers per section. The mean fluorescence intensity (MFI) was quantified for immunostaining of CEND1, H3K4me1, H3K4me2, H3K9me1, and H3K9me2.

Isolation and culture of primary neonatal rat or mouse cardiomyocytes

Neonatal rat and mice cardiomyocytes (NRCMs and NMCMs) were isolated from P3 pups. Briefly, ventricles were dissected out from P3 neonatal rat or mouse, then minced and digested with 0.2% collagenase type II (Worthington, LS004176) at 37°C. Non-cardiomyocytes including cardiac fibroblasts were removed by adhesive plating for 2 h. Purified cardiomyocytes were cultured in Dulbecco's modified Eagle's minimum essential medium (DMEM) (Gibico, C11965500BT) supplemented with 20% FBS (BI, 1706126) and 1% Penicillin/Streptomycin at 37°C in a cell culture incubator. To inhibit LSD1 activity, the NRCMs and NMCMs cells were treated with 250 nM and 500 nM of GSKLSD1 (Sigma, SML1072), respectively. To overexpress LSD1, NRCMs were infected with adenovirus carrying human *LSD1* gene. For the rescue experiments, cells were infected with lentivirus carrying *Cend1* shRNA to knock down the expression of *Cend1*. Additionally, H9C2 cells were cultured in DMEM media containing 10% of FBS and treated with 500 nM of GSKLSD1.

Generation and culture of ihPS-CMs

Cardiomyocyte differentiation was performed in a growth factor and serum-free medium. hiPSCs was treated by the GiWi protocol-modulate the canonical Wnt signaling pathway with GSK3 inhibitor (Gi) and Wnt inhibitor (Wi). Briefly, hiPSCs was harvested using 0.5mM EDTA when the confluence was 80-90%. The specific maintaining medium was added to resuspend hiPSCs to make it at 0.5 x 10^5 cells/ml. The cell suspension was seeded in a 12-well matrigel-coated plate (2ml/well) at minus day4. At day 0 the medium was changed with RPMI/B-27 medium containing CHIR99021 (10 μM, GSK3 inhibitor) without insulin and incubated for 24 h. The medium was renewed with RPMI/B-27 medium without insulin for 48 h. On day 3 of the hiPSCs differentiation, the medium was replaced with RPMI/B-27 medium containing IWP2 (5 μM, Wnt inhibitor) without insulin for 48 h, followed by RPMI/B-27 medium without insulin for 72 h. From day 7, hiPSC was cultured with RPMI/B-27 medium containing insulin and refreshed the medium every 3 days. On day 8, hiPSCs could beat rhythmically. The differentiated hiPSCs was treated with 1 μM GSKLSD1.

RNA-seq data analysis

Sequencing reads generated from the Illumina platform were assessed for quality using Fastp (version 0.23.1)[44] with the following filtering criteria: (1) Discard a paired reads if either one read contains adapter contamination; (2) Discard a paired reads if more than 10% of bases are uncertain in either one read; (3) Discard a paired reads if the proportion of low quality (Phred quality <5) bases is over 50% in either one read. The clean data was used for next mapping step and aligned to the mouse reference genome (GRCm39) using the Hisat2 (v2.0.5).[45] FeatureCounts (v1.5.0-p3)[46] was used to count the reads numbers mapped to each gene using the annotation file (Mus_musculus.GRCm39.109.gtf) and then FPKM of each gene was calculated based on the length of the gene and reads count mapped to this gene. For differential expression analysis, data analysis with the DEseq2 package[47] in R 4.2.1 and the resulting *p* values were adjusted using the Benjamini and Hochberg's approach for controlling the false discovery rate. Genes with fewer than 50 counts were filtered out first in

each sample, then padj ≤ 0.05 and |log2 (foldchange)| ≥ 0.5 were set as the threshold for significantly differential expression. Gene Ontology (GO) and KEGG pathways enrichment analysis of differentially expressed genes were done with the clusterProfiler package (R 4.2.1)[48] in which gene length bias was corrected. GO and KEGG terms with corrected $p < 0.05$ were considered significantly enrichment. Gene Set Enrichment Analysis (GSEA) of the complete pre-ranked gene list was carried out using the GSEA_4.1.0 software and the Hallmark gene set collection within the Molecular Signatures Database (MSigDB).

Quantitative reverse transcription PCR (qRT-PCR)

Total RNAs were extracted from ventricles or cultured cardiomyocytes using TRIzol reagent (Sigma). An amount of 1 μg of total RNA was reverse transcribed to cDNA using HiScript II reverse transcriptase (Vazyme, R222). qRT-PCR involved using SYBR Green PCR Master Mix (Genstar) on Quant gene 9600 Fast Real-Time PCR System. Target genes were amplified with gene specific primers (Table S2). The expression of target genes was normalized to that of *Gapdh* or *β-actin* and calculated by using the $2^{-\Delta\Delta CT}$ method. Biological replicates were performed using at least three individual samples.

Western blot

The total protein was isolated from ventricles or cultured cardiomyocytes with RIPA lysis buffer (Servicebio, G2002) and quantified by bicinchoninic acid assays. Equal amounts of total proteins were separated in SDS-PAGE gels and transferred onto polyvinylidene fluoride membranes (Roche, ISEQ00010). The membranes were blocked with 5% BSA (Millipore, FC0077) for 1 h at room temperature, then incubated with primary antibodies at 4°C overnight. After three washes with TBST, the membranes were incubated with HRP-conjugated secondary antibodies for 1 h at room temperature. After three washes of TBST, the membranes were exposed with enhanced chemiluminescence (Vazyme, E411-04).

Plasmid construction and lentivirus package

For *Cend1* knockdown, shRNA or sgRNA were designed (mouse *Cend1* shRNA: CATAGCTCTAATTCTTGGTGT; rat *Cend1* shRNA: CCGTACTTCTCAACAATCATT; human *CEND1* sgRNA: CCACTTCCTGTACAGACCCG. CTL shRNA: GTACGTACGTACGTACGTACT) and inserted into the pLKO.1 lentivirus vectors. In brief, the oligos of target shRNA were produced by annealing and inserted into pLKO.1 vector with T4 DNA ligase (NEB, M0202). After transformation into competent DH5 alpha cells, the plasmids were extracted with TIANprep mini plasmid kit (Tiangen, DP103) and the sequence was confirmed by Sanger sequencing. For lentivirus production, the packaging vectors pSPAX2 and pDM2G were co-transfected with Control (pLKO.1-shCTL vector) or target plasmids (pLKO.1 vector containing the shRNA or sgRNA sequence) into the HEK-293T cells by using Lipfiter3.0 Transfection Reagent (HanBio, China, HB-TRLF3), with the DNA ratio (target plasmid: pSPAX2: pDM2G = 4:3:1) used. The culture media containing virus was harvested at 48 and 72 h after transfection, and underwent centrifugation at 1250 rpm for 5 min at 4°C, then the supernatant was transferred to a new tube, aliquoted and stored at -80 °C for long-term storage. Indicated cells were infected with the mix of medium and lentivirus with 10 μg/ml polybrene, then infected cells were selected by 1 μg /mL puromycin for 24-48 h (Sigma, P9620). The mRNA expression of *Cend1* were evaluated by RT-qPCR assay to verify the knock-down efficiency.

ChIP-qPCR

ChIP-qPCR assays were performed using the SimpleCHIP Enzymatic Histone IP kit (Cell Signaling Technology, 9003) according to the manufacturer's protocols. First, H9C2 (1*10^7 cells) were fixed with 1% formaldehyde (Sigma, 252549) for 10 min at room temperature to crosslink protein and DNA complexes. Then cells were quenched with 1.5 M glycine. After three washes with PBS, cells were sonicated to shear DNAs into 100–300 bp fragments. The DNA fragments were incubated with 5 μg antibodies against H3K4me2 (Abcam, ab32356, 1:100) overnight at 4°C using magnetic beads in a final volume of 500 μl. The normal rabbit immunoglobulin (IgG) in the kit was used as negative control. Immunoprecipitated DNA was extracted and used for qPCR analysis to determine the enrichment of DNA fragments containing the CEND1 promoter with specific primers.

Luciferase reporter assay

Luciferase reporter assays were performed to evaluate the *Cend1* promoter activity regulated by LSD1. A 1-kb promoter of murine *Cend1* gene was amplified by PCR and cloned into the pGL3-basic vector to generate the plasmid pGL3-*Cend1*P. First, the HEK-293T cells were seeded into 12-well plates and transfected with pGL3-*Cend1*P and pRL-TK by using Lipofectamine 2000 Reagents (Invitrogen, 11668019). Then cells were treated with 250 nM GSKLSD1 or AdLSD1 virus 12 h after transfection. Finally, the cell lysates were collected and subjected to luciferase reporter assays with Dual-luciferase reporter assay system (Promega, E1980). Luciferase activities were calculated as firefly luciferase normalized to Renilla luciferase luminescence.

QUANTIFICATION AND STATISTICAL ANALYSIS

Statistical analysis

All data were presented as mean ± SEM. Statistical analysis was performed using GraphPad Prism software. The Student *t* test was used for comparison between two groups. One-Way ANOVA with Tukey tests was performed for comparisons among three groups. Difference was considered as statistically significant when p value < 0.05 (*), p value < 0.01 (**), p value <0.001 (***).